PHYSICAL REVIEW B VOLUME 18, NUMBER 8 15 OCTOBER 1978

# Optical properties of the sodium-tungsten bronzes and tungsten trioxide

J. F. Owen and K. J. Teegarden
*Institute of Optics, University of Rochester, Rochester, New York 14627*

H. R. Shanks
*Ames Laboratory-United States Department of Energy, Iowa State University, Ames, Iowa 50011*

(Received 6 March 1978; revised manuscript received 1 June 1978)

A polarization-modulation ellipsometric technique was used to make direct measurements of the optical dielectric constants of single-crystal specimens of the nonstoichiometric tungsten-bronze compound $Na_xWO_3$ ($0.52 < x < 0.94$) and $WO_3$, in the energy range from 1.0 to 5.5 eV. A method for determining the optical constants of anisotropic materials from modulation ellipsometry was developed in the study of tungsten trioxide. The behavior of the sodium bronzes as a function of sodium concentration is in agreement with recent calculations of the band structures for these materials. The system exhibits almost rigid-band behavior. The data were fit to the classical Drude free-electron model for the optical properties of metals. The $WO_3$ dielectric constants were used to directly determine the contribution of higher-energy bound-electron transitions to the optical constants of $Na_xWO_3$ in the free-electron region. The results of joint-density-of-states calculations were used in conjunction with the free-electron model to demonstrate that a relatively large discrepancy between conduction-electron relaxation times derived from the free-electron model alone and those determined from the dc conductivity may result, in part, from underlying interband transitions.

## I. INTRODUCTION

The tungsten bronzes, a group of nonstoichiometric solid solutions of general chemical formula $M_xWO_3$, where $M$ is typically an alkali metal, have many physical properties which are of both practical and fundamental significance.[1] Only recently have many of these properties, such as superconductivity and ferroelectricity, become known. As a result, there has lately been an increased amount of experimental work done on the bronzes, some of which has involved the use of optical techniques to investigate these materials.[2-12]

The first optical measurement on bronze-related single-crystal samples was the reflectivity spectrum of $ReO_3$ from 0.1 to 22 eV obtained by Feinleib, Scouler, and Ferretti.[7] Kramers-Kronig analysis of the spectrum was performed in order to determine the real and imaginary parts of the optical dielectric constant. Later studies were made on $ReO_3$ by Weaver and Lynch[8] and on $Na_xWO_3$ by Consadori and Stella[9] and Giuliani *et al.*[10] Lynch *et al.*[11] measured the reflectivity of two cubic sodium bronzes ($x = 0.65$ and $x = 0.735$) and one tetragonal potassium bronze ($x = 0.63$) from 0.1 to 38 eV and obtained the optical constants over that range by Kramers-Kronig analysis. The spectra were interpreted in terms of the band structure of $ReO_3$, a structurally similar compound. Most recently there has been a study of $Na_xWO_3$ ($x = 0.52, 0.72, 0.85$) by Camagni *et al.*[12] employing standard ellipsometric techniques from 0.3 to 5.2 eV and electromodulated reflectance from 1.3 to 3 eV. Drude and Lorentz models were used to determine the free- and bound-electron components of the ellipsometric data. The electroreflectance data were explained via a model involving a modulation of the optical constants in a thin surface layer of the metal and in terms of the $ReO_3$ band structure. The ellipsometric data are in substantial agreement with our work, although the analysis in terms of the Drude and Lorentz models differs.

In this work we have made further measurements of the real and imaginary parts of the dielectric constants of cubic $Na_xWO_3$ and have included measurements on $WO_3$ to permit a direct determination of the contribution of bound electrons to the dielectric constants. Measurements were carried out on single-crystal specimens using a modulation ellipsometric technique which yields the optical constants directly, without the need for Kramers-Kronig analysis. The results support the rigid-band model for these materials. A least-squares fit of the data to a modified Drude free-electron model yields the free-electron effective mass and relaxation time as a function of composition. A discrepancy between the values of the relaxation times determined from the optical data and those obtained from the dc conductivity is observed. Using recently performed joint-density-of-states calculations for the sodium-bronze system[13] it is demonstrated that direct transitions within the conduction-band manifold could, in part, account for this discrepancy.

 

## II. EXPERIMENTAL

The technique used to measure the optical constants was a type of polarization modulation ellipsometry developed by Jasperson and Schnatterly.[14] Chopped, monochromatic, collimated, linearly polarized light is passed through a photoelastic device which modulates the polarization of the light by introducing a varying phase shift between the perpendicular components of the linearly polarized light. The modulated light is reflected from the sample at a convenient angle of incidence, 45° in this case, into a photomultiplier. Two measurements are made, one with the initial polarization in the plane of incidence of the sample, and one with the initial polarization at 45° to the plane of incidence. In the second case a linear analyzer follows the sample. The output of the photomultiplier is fed into two lock-in amplifiers, one which measures the amplitude of the signal at the chopped frequency (giving the total light intensity), and one which measures the amplitude of the signal at either the fundamental or first harmonic of the modulation frequency. The outputs from the lock-in amplifiers are fed into a ratiometer. From these two measurements, knowing the modulation depth, the optical constants of isotropic samples can be calculated in the manner described by Jasperson and Schnatterly.[14]

Since noncubic media are optically anisotropic, determination of the optical constants is more complicated than in cubic materials. (Aside from the reflectivity spectrum of $K_{0.63}WO_3$ by Lynch *et al.*,[11] the only previous optical constant measurements on a noncubic tungsten-bronze material has been the determination of the indices of refraction of $WO_3$ in white light by Sawada and Danielson.[15]) In order to calculate three sets of optical constants for $WO_3$, which is biaxial, a formalism presented by Graves[16] was employed. The technique involves mathematical iterations using results from three sets of ellipsometric measurements on faces perpendicular to the principal axes of the crystal.

The modulator in the apparatus is a modification of one built by Chabay, Hsu, and Holzwarth[17] and used to measure circular dichroism in the infrared. The main difference is that their germanium optical element is replaced with high-grade fused silica. The entire modulator assembly is a 2.5×2.5×30-cm bar consisting of seven sections cemented end to end. The optical element, 7.5 cm in length, is the central unit, situated between two 3.5-cm long stainless-steel blocks. A 0.75×2.5×2.5-cm PZT (lead zirconate titanate) piezoelectric element is cemented between each of these blocks and the 7.0-cm long stainless-steel end pieces. The fundamental longitudinal acoustical mode of the bar is excited by electrically driving the PZT disks at the resonant frequency of the bar, approximately 6 kHz. The bar is kept on resonance with a feedback circuit which detects the relative phases of the current and voltage applied to the tranducers and adjusts the driving frequency so as to keep them in phase. The light beam passes through the silica element initially polarized at 45° to the long axis of the bar (the strain axis) and polarization modulation results from the strain-induced change in the index of refraction along that axis.

$Na_xWO_3$ samples were grown by electrolysis from a fused salt melt.[18] Using seed crystals as the cathode, large single crystals with usable surfaces of 0.5–1 $cm^2$ were obtained. Sodium concentrations for the samples were calculated from the lattice constants using the expression $a = 0.0818x + 3.7850$ Å determined for $Na_xWO_3$ from neutron-activation analysis[19] and x-ray diffraction.[2] Lattice constants were measured by x-ray diffraction using a Debye-Scherrer powder camera. The tungsten trioxide sample, prepared by vapor transport,[20] was a $c$-axis platelet having dimensions of 2×2×1 mm.

The samples were mounted in "Quickmount," a commercial plastic mounting compound, and mechanically polished in a conventional fashion on silk and cloth covered wheels using progressively finer grits. The final polish was done with 0.05-$\mu$m alumina, yielding mirrorlike surfaces. Samples were cleaned ultrasonically in methanol followed by distilled water. All optical measurements were completed within 3 h after the final polishing of the samples. The data presented were taken at room temperature with the sample surfaces exposed to air. However, measurements made on samples which were polished and maintained in an argon atmosphere in order to avoid oxidation of the surfaces yielded no significant difference in the results.

## III. RESULTS

### A. $Na_xWO_3$

The optical dielectric constants of the cubic sodium tungsten bronzes, $Na_xWO_3$, for $x$ values of 0.522, 0.628, 0.695, 0.740, 0.805, 0.860, and 0.940 are shown in Fig. 1.

The general shapes of the curves are strikingly similar, an indication of the "rigid-band" nature of the compounds.[21] Two distinct regions are apparent in the data. At long wavelengths, from 1.2 to around 2.5 eV, the dielectric constants exhibit typical free-electron-like behavior. $\epsilon_1$ increases

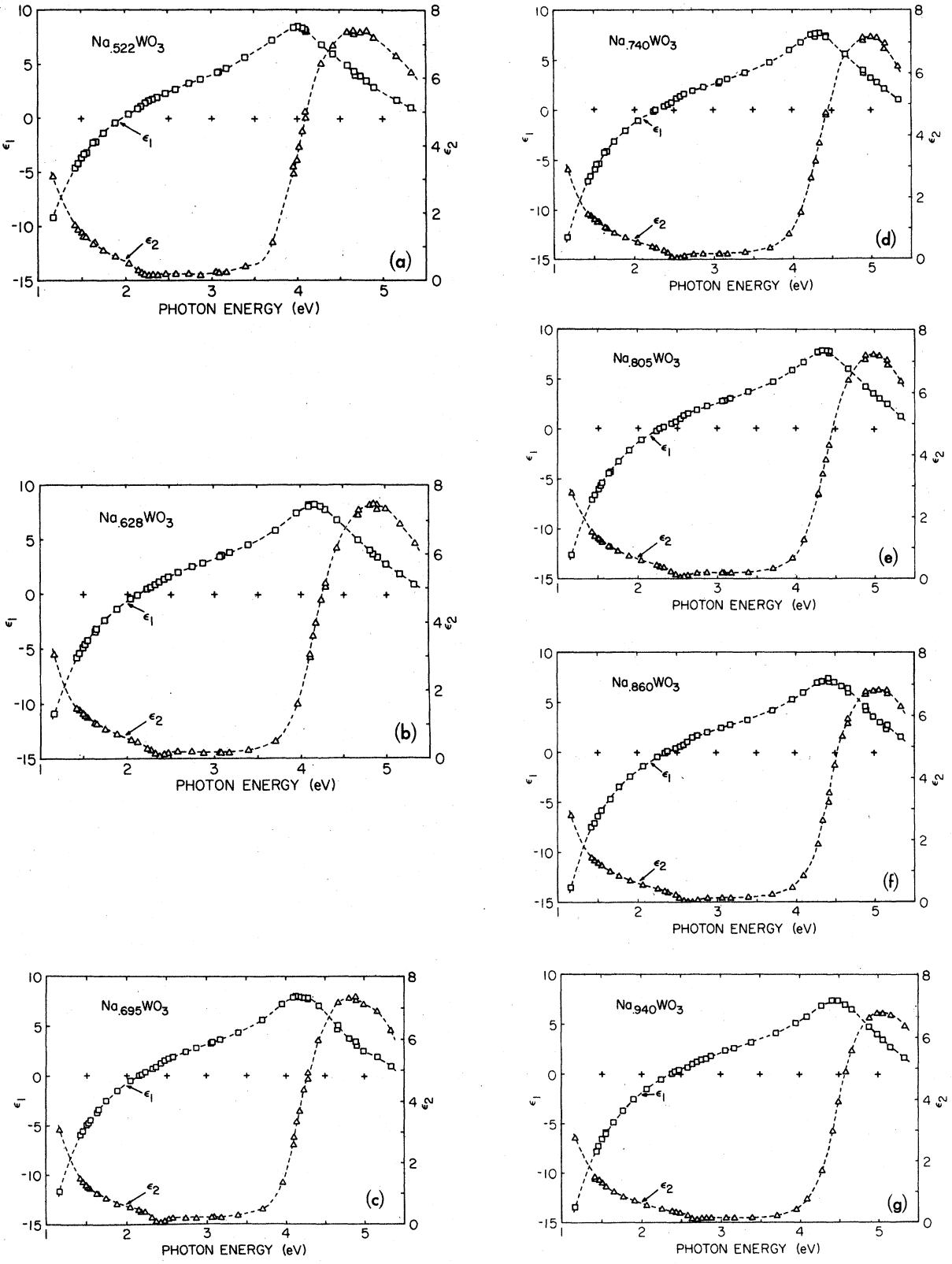


FIG. 1. Real and imaginary parts of dielectric constants of $Na_xWO_3$.

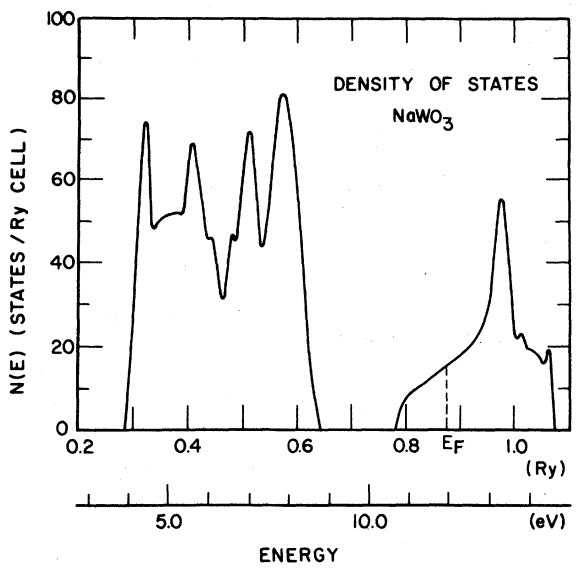


FIG. 2. Density of states in $NaWO_3$ calculated by Kopp *et al.* (Ref. 21).

from a large negative value, crossing zero at the "screened" plasma frequency, while $\epsilon_2$ decreases from a large positive value, becoming asymptotic to zero. At the short-wavelength end of the spectrum structure appears which bears a resemblance to a single oscillator Lorentz transition. The imaginary part of the dielectric constant $\epsilon_2$ peaks at the resonant frequency, around 5 eV, while $\epsilon_1$ shows dispersive behavior about the transition energy.

As $x$ increases, a definite shift in the uv structure toward higher energy is observed. The cause of this shift is evident from consideration of the band structure of the bronzes. The band structure of $Na_xWO_3$ is similar to that of $ReO_3$. The top of the valence band is made up primarily of oxygen $p$ orbitals while the conduction band, predominantly $d$-like in nature, results from covalent $\pi$ bonding between the oxygen $2p$ and the tungsten $5d$ orbitals.[21-25] A sketch of the density of states in $NaWO_3$, from recent band-structure calculations,[21] is shown in Fig. 2. The value of $\epsilon_2$ in the uv data is determined primarily by transitions from states at the top of the valence band to states above the Fermi level in the conduction band. Because of the rigid-band nature of the system, the density of states in the cubic bronzes with $x$ less than 1 is almost identical to that shown. The Fermi level varies from the center of the band gap, for $x = 0$, to the dotted line shown in the figure, for $x = 1$. Since the Fermi level rises with increasing electron concentration, the onset of these transitions shift to higher energies as sodium is added to the system. The position of the peak in $\epsilon_2$ at 5 eV corresponds to the energy difference between the peak in the density of states at the top of the valence band and the peak above the Fermi level in the center of the conduction band. If the system were a perfect rigid-band system the position of the peak in $\epsilon_2$ would not change with composition. However, Coulomb repulsion within the filled states in the conduction band causes the energy of these bands to increase with increasing occupation.[21] Thus the band gap widens as sodium is added to the lattice, giving rise to the observed shift of the optical data toward shorter wavelengths.

In the long-wavelength region of the spectrum, the Drude region, a shift in the optical data toward higher energies with increasing $x$ values is also apparent. The origin of this shift is twofold. In the free-electron model, $\epsilon_1$ decreases and $\epsilon_2$ increases with increasing free-electron concentrations. Thus one contribution to the shift is the change of free-electron density with sodium concentration. However, there is also a contribution to $\epsilon_1$ in this energy range from the 5-eV bound-electron transition. As the transition moves to higher energies with increasing sodium concentration, its contribution to $\epsilon_1$ in the long-wavelength region decreases and causes the curve to shift to higher energies.

In a free-electron metal, at a photon energy where $\epsilon_1 = 0$ and $\epsilon_2$ is small, a large optical absorption occurs. This energy corresponds to the "plasma frequency," at which a bulk longitudinal plasma resonance could occur. For a completely-free-electron system with an electron concentration equal to that of the cubic tungsten bronzes the plasma frequency would occur in the ultraviolet, arount 4 eV. However, the contribution to $\epsilon_1$ from the bound transition at 5 eV has shifted the point at which $\epsilon_1$ crosses zero to the middle of the visible wavelength region. Since $\epsilon_2$ is small here, plasma resonance behavior occurs. At energies below the plasma frequency, the reflectivity is high. At wavelengths close to the plasma frequency, the reflectivity falls off sharply. The material would become transparent above the plasma frequency were it not for the absorption due to higher-energy transitions. A plot of the absorption peak (reflectivity minimum) and plasma energy as a function of sodium concentration is shown in Fig. 3. Also shown for comparison are values obtained by other authors. The values of $\omega_p$ of Camagni *et al.*[12] are lower than those of this work because these authors present the energies at which the $\epsilon_1$ function fitted to their data is equal to zero, rather than the energy at which the

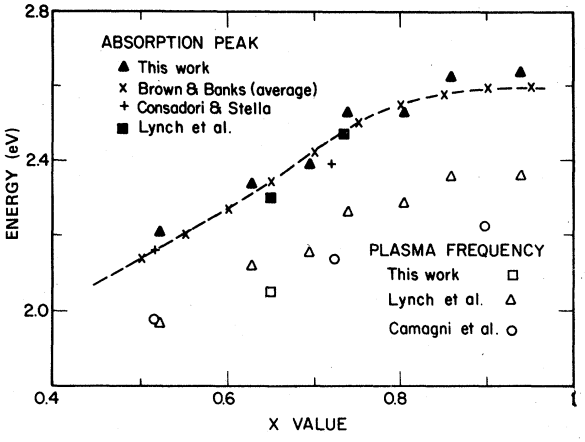


FIG. 3. Screened plasma frequency ($\epsilon_1$ zero crossing) and associated absorption peak vs composition in $Na_xWO_3$. Values obtained from direct reflectivity measurements (Ref. 2, 9, and 11) and ellipsometry (Ref. 12) by other authors are shown for comparison.

$\epsilon_1$ data is equal to zero. An anomaly in their data in this region obscures the actual zero crossing.

### B. $WO_3$

The dielectric constants of tungsten trioxide are shown in Fig. 4. The $WO_3$ data is quite similar to that of $Na_xWO_3$, but does not show a free-electron contribution. This, in fact, is just what would be expected for a rigid-band system. The sodium atoms play little role in the electronic band structure other than, indirectly, by changing the energy of the conduction band via Coulomb repulsion in filled states and, perhaps, by changing the lattice parameters. It is the same valence- to conduction-band transition which gives rise to the structure at 4 eV in $WO_3$ that is responsible for the uv structure in the $Na_xWO_3$ data. The onset of the transition in $WO_3$ is shifted to a lower energy, in keeping with the behavior found in the tungsten bronzes.

In order to determine the optical constants of a biaxial crystal it is necessary to make multiple ellipsometric measurements. Using the technique of Graves,[16] the dielectric constants can be determined from three measurements: two on a surface perpendicular to one optical axis, with the sample rotated 90° about that axis in the two cases, and a third on a surface perpendicular to the second optical axis. In order to check the consistency of our results, two sets of measurements were performed on each surface, thus allowing two sets of optical constants to be calculated from the two triplets of data. Although the two sets of dielectric constants were similar, slight differences between them indicate an inconsistency in the measurements or data reduction. This may be a result of the nature of the sample. The $WO_3$ sample is a small platelet with the $c$ axis perpendicular to the plate. Although the natural faces on the sides of the plate are 100 faces, investigation with a polarizing optical microscope indicates the existence of a number of domains, having two different orientations, 90° from each other. These are evidently ferroelectric domains, having reversed $a$ and $b$ axes. Thus, optically, the sample does not behave as a true single crystal. The ellipsometric measurements are probably being influenced by contributions from domains with differing crystallographic orientations, giving rise to the observed discrepancies. This would also explain the double peaks which appear in the $WO_3$ $\epsilon_2$ data, but do not occur in the $Na_xWO_3$ results. If the double peaks were "real" they would indicate a splitting in the states which give rise

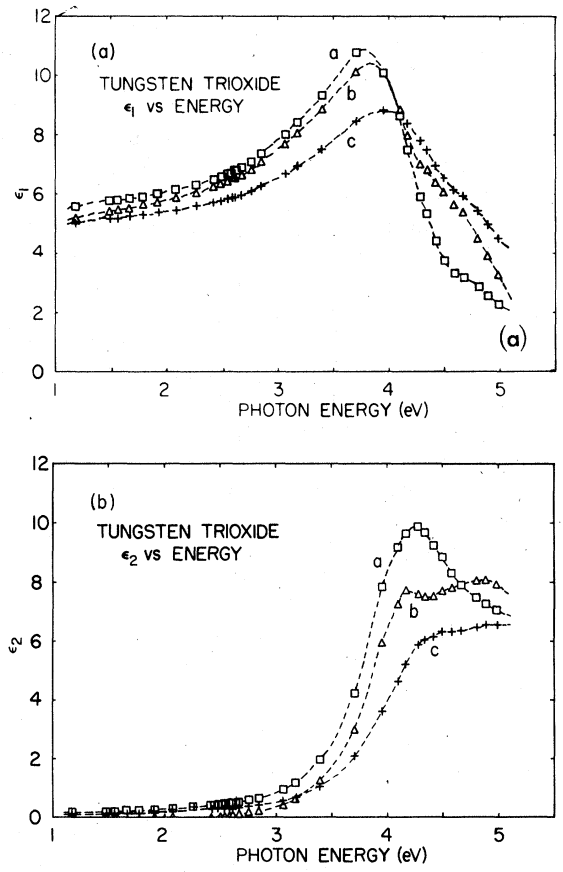


FIG. 4. (a) Real part of the dielectric constant for the $a$, $b$, and $c$ axes of $WO_3$. (b) Imaginary part of the dielectric constant of $WO_3$.

to the transition. Although it is possible that the lower symmetry of $WO_3$ causes such a splitting, it is more likely that, because of the different lattice constants in the monoclinic structure, the position of the peak in $\epsilon_2$, the transition energy, differs for the three principal axes. The double peaks appear in the ellipsometric results because domains of differing orientations make contributions to the measured signal which is interpreted in the analysis as data corresponding to only one orientation.

The only optical measurements on $WO_3$ available for comparison with our data are the indices of refraction in white light made by Sawada and Danielson[15] using a modified Chaulnes method. Their results are in reasonable agreement with the values found in the visible region in this work.

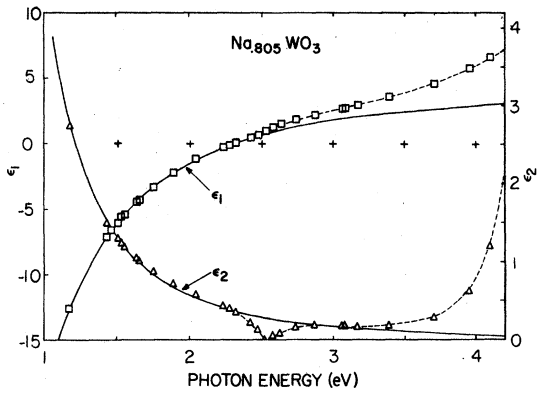


FIG. 5. Least-squares fit of the Drude free-electron model to the $Na_{0.805}WO_3$ optical data.

## IV. ANALYSIS

### A. Drude free-electron model

The most straightforward manner in which to interpret the free-electron portion of the tungsten-bronze data is to fit the real and imaginary parts of the dielectric constant, $\epsilon_1$ and $\epsilon_2$, directly to the Drude free-electron model. From the $\epsilon_2$ spectra of $Na_xWO_3$, it can be seen that the contribution to the imaginary dielectric constant from the higher-energy transitions is negligible in this region. The resonant peak is clearly separated from the Drude region of the spectrum by a region of low $\epsilon_2$. However, contributions to $\epsilon_1$ from interband transitions extend over a much wider energy range than is the case for $\epsilon_2$. In order to simplify the situation, it is reasonable to assume that, in the case of $Na_xWO_3$, the contribution in the Drude region from the 5-eV transition is constant as a function of wavelength. The validity of this assumption will be demonstrated in Sec. IV C using the optical data of $WO_3$ to determine the contribution directly.

The expressions used in the model are the standard Drude functions with the inclusion of an effective mass and a constant term in $\epsilon_1(\omega)$ to account for higher-energy transitions:

$$\epsilon_1(\omega) = 1 - \omega_p^2/(\omega^2 + 1/\tau^2) + \epsilon_1^b , \tag{1}$$

and

$$\epsilon_2(\omega) = \omega_p^2/\omega\tau(\omega^2 + 1/\tau^2) , \tag{2}$$

where $\omega_p^2 = 4\pi Ne^2/m^*$. The fitting parameters of the model are $m^*$ the effective mass, $\tau$ the electron relaxation time, and $\epsilon_1^b$ the contribution to $\epsilon_1$ from higher-energy transitions. The number of electrons per unit volume $N$ was calculated from the lattice constants, assuming one free electron per sodium atom. The fitting was done using MLAB, a computer modeling and graphics program, developed by the National Institutes of Health, which employs the Marquardt-Levenberg least-squares fitting method.

The data used in the analysis extend from 1.0 to 2.4 eV. The $\epsilon_1$ and $\epsilon_2$ data were fit to their respective functions simultaneously. Figure 5 shows a typical least-squares fit of the data, in this case for $Na_{0.805}WO_3$, to the free-electron model. The parameters obtained from the fitting procedure for $Na_xWO_3$ are plotted versus sodium concentration in Fig. 6.

Figure 6(a) shows $\epsilon_1^b$ versus sodium concentration. Although it is impossible to compare the absolute values of the results to any theoretical values without specific details of the transitions which give rise to $\epsilon_1^b$, the results show the expected qualitative behavior. The transition near 5 eV moves to higher energies with increasing sodium concentration as a result of Coulomb repulsion in the filled states. The contribution to $\epsilon_1$ in the long-wavelength region decreases as the transition moves farther away. Consequently, $\epsilon_1^b$ decreases as $x$ increases.

Similarly, a qualitative argument can be made concerning the electron effective-mass ratio, shown in Fig. 6(b). As the Fermi level rises in the conduction band, larger portions of the Fermi surface will have negative curvature. In these regions the inverse effective-mass tensor is negative. Thus, the average inverse mass tensor decreases and the effective mass increases with a rising Fermi level, in agreement with the optical data. This effect has also been noted in connection with the increase in the Hall coefficient with increasing sodium concentration in $Na_xWO_3$.[26] Another argument is given by Goodenough,[24] who suggests that the conduction-band ($\pi^*$ band) band-

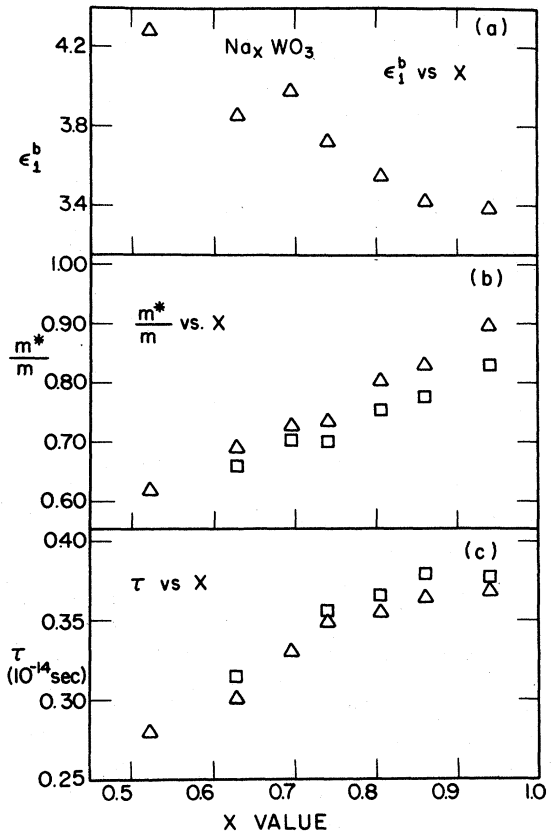


FIG. 6. Contribution to $\epsilon_1$ from high-energy transitions (a) effective-mass ratio (b) and electrons relaxation time (c) vs composition for $Na_xWO_3$ as determined from the Drude free-electron models. The triangles represent the model in which $\epsilon_1^b$ is included as a frequency-independent fitting parameter, while the squares represent the model in which $\epsilon_1^b(\omega)$ is determined directly from $WO_3$ optical data.

width decreases with increasing $x$, giving rise to a decreasing effective mass. The narrowing of the band results from competition of the sodium-oxygen $\sigma$ bonding with the tungsten-oxygen $\pi$ bonding as the concentration of sodium increases. This narrowing of the bandwidth is not evident in the band-structure calculations of Kopp *et al.*[21] Although the optical effective-mass ratios found are low compared to values ranging between 1 and 3 which have been determined for the density of states effective mass using magnetic susceptibility,[27] transport,[28] specific heat,[29] and electroreflectance[10] measurements, they are comparable to an optical mass of 0.86 found for $ReO_3$,[7] and 0.5 found for $Na_{0.5}WO_3$,[4] using a similar analysis on reflectivity data.

In Fig. 6(c) is shown the relaxation time versus composition obtained from the fitting procedure. Again, the expected qualitative behavior is apparent. At room temperature the relaxation time is primarily a function of phonon scattering, which should be fairly independent of composition. However, impurity scattering does play a small role in the room-temperature resistivity of the sodium bronzes, as is evident from the conductivity measurements of Muhlestein and Danielson.[26] Their work shows the effect of sodium ordering, which generally increases as $x$ increases above 0.5, on the electrical conductivity. Although the effect is much more drastic at liquid-helium temperatures, it is still apparent at room temperature. As the ordering increases, the relaxation time should also increase. Unfortunately, in the present work the resolution of the fitting scheme is not sufficient to observe the anomaly seen by Muhlestein and Danielson at $x = 0.75$.

Although the qualitative behavior of $\tau$ is correct, the results do not agree quantitatively with dc measurements. Using the relation $\sigma = Ne^2\tau/m^*$, $\tau$ calculated from the data of Muhlestein and Danielson[26] varies from $0.45\times10^{-14}$ sec at $x = 0.52$ to $1.1\times10^{-14}$ sec at $x = 0.86$, compared to $0.28\times10^{-14}$ sec to $0.36\times10^{-14}$ sec for the corresponding compositions in this work. Thus the relaxation times found from the Drude model are a factor of 2 or 3 below the values expected from the dc measurements. A similar discrepancy has been noticed in a calculation of the relaxation time from $ReO_3$ optical data.[7] The only $Na_xWO_3$ optical data for comparison are those of Camagni *et al.*[12] who present values for $\gamma = 1/\tau$ obtained from a similar fit of their optical data to the free-electron model. Evidently a misprint appears in the report, for in order to obtain their calculated curves using their parameters, $\gamma$ must be multiplied by a factor of 10. Values of $\tau$ calculated from their values of $\gamma$, after making this correction, are lower than those of this work by approximately a factor of 2, in even greater disagreement with predictions based on the dc conductivity. The relatively large discrepancy between dc and optical relaxation times raises the possibility that the optical data in the "free-electron" region are, in fact, being affected by underlying direct interband transitions, even though no structure in the data is apparent. This possibility will be explored in the following section.

### B. Direct transitions in the "free-electron" region

In metals the relaxation times calculated from dc conductivity are frequently found to be larger than those calculated from optical data using the classical free-electron model.[7,30-33] A number

of arguments are generally invoked to explain these discrepancies.[34] It was first pointed out by Holstein[35] that quantum effects cause the relaxation time resulting from electron-phonon interactions to be frequency dependent. The effect is particularly important at low temperatures where there are few phonons present to be absorbed in interactions and only electrons which have gained sufficient energy via optical excitation can give rise to phonon emission. A frequency-dependent relaxation time can also result from electron-electron interactions,[36] which, although insignificant in the case of dc resistivity, can become important at optical frequencies. Calculations using the relations presented by Abèles[34] indicate that for the cubic sodium-tungsten bronzes electron-electron effects are negligible and the quantum effects should give rise to a difference of approximately 30% between relaxation times calculated from dc and optical data in the red and near infrared. Finally, a discrepancy between the optical and dc relaxation times also arises if the relaxation time of the electrons is not isotropic over the Fermi surface. The relaxation time obtained from dc measurements is essentially the average of $\tau$ over the Fermi surface, whereas optical data yield the average of $1/\tau$ over the Fermi surface. Unless $\tau$ is constant, $\langle\tau\rangle > \langle 1/\tau\rangle$. Although the magnitude of this effect would be difficult to calculate for the bronzes, at room temperature this typically gives rise to a dc relaxation time which is larger than the optical relaxation time by a factor of 1.5.[34] Thus, it appears that the discrepancy observed in the bronzes is somewhat larger than is expected from the above considerations.

There is, however, another factor that should be considered, particularly in the case of the bronzes, which may contribute substantially to such a discrepancy. Low-energy direct transitions, which are not taken into account in the free-electron model, can occur within the conduction band of a metal. Low-energy interband transitions have been observed in $ReO_3$, an electronically similar compound, by Weaver and Lynch[8] using a calorimetry technique to measure absorption. These transitions were attributed to degenerate bands crossing the Fermi level which are split by spin-orbit interactions. The resulting bands are nearly parallel and give rise to a large joint density of states. Previous reflectivity measurements had not revealed the structure, which is masked by the free-electron reflectivity. An analysis of the $ReO_3$ infrared data in terms of the free-electron model by Feinleib *et al.*[7] led to an optical relaxation time of $0.29\times10^{-14}$ sec, comparable to the values found for $Na_xWO_3$ in this

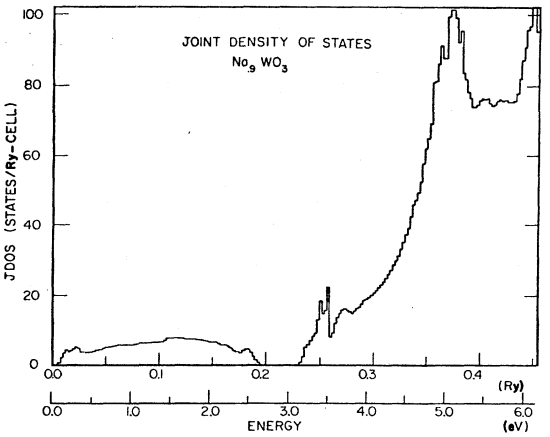


FIG. 7. Joint density of states for $Na_{0.9}WO_3$ calculated by Harmon (Ref. 13).

work. This is a factor of 3 below that expected from the dc conductivity. No definite structure in optical data attributable to low-energy interband transitions has been observed in the cubic sodium bronzes, although the possibility has been suggested.[11]

Recently, joint density of states (JDOS) calculations for the $Na_xWO_3$ system have been made by Harmon.[13] The results of the calculations for $x = 0.9$ are shown in Fig. 7. Two distinct regions are apparent in the figure. From 0 to about 2.6 eV the contribution to the JDOS is from states within the $t_{2g}$ conduction band. Given nonzero matrix elements, these transitions would contribute to the optical constants in the Drude region. There is a 0.6-eV gap between these states and the onset of valence-to-conduction band transitions, possibly combined with transitions between the $t_{2g}$ and $e_g$ manifolds of the conduction band, which begin around 3.2 eV. There is a peak at 5 eV which corresponds to the peak at the same energy observed in the ellipsometric optical data.

With the aid of JDOS calculations it is possible to add to the free-electron model contributions to the optical constants from underlying direct transitions within the conduction band. If the dipole matrix element is approximately constant for such transitions the contribution to the imaginary part of the dielectric constant from the transitions can be approximated as

$$\epsilon_2^d(\omega) = C|M_{if}|^2 J(\omega)/\omega^2 , \tag{3}$$

where $M_{if}$ is the dipole matrix element, $J(\omega)$ is the joint density of states, and $C$ is a constant. It was necessary, in this case, to insert the matrix element for these transitions in our model as a variable parameter since no calculations of the

matrix elements for these transitions in the bronzes are available. Because the transitions are all within the same set of bands it is reasonable to assume that the matrix element is roughly a constant. The expression used to fit the $\epsilon_2$ data in the long-wavelength region is obtained by combining Eqs. (2) and (3):

$$\epsilon_2(\omega) = \frac{\omega_p^2}{\omega\tau(\omega^2 + 1/\tau^2)} + C|M_{cc}|^2 \frac{J(\omega)}{\omega^2}, \qquad (4)$$

where $M_{cc}$ is the matrix element for transitions within the conduction band. The interband contributions to $\epsilon_1$ were not included in the model because of the small influence this would have on the parameters obtained and on the conclusions drawn from the analysis.

In order to determine whether values obtained for $M_{cc}$ are reasonable, it is possible to compare them with the matrix element $M_{vc}$ for the valence- to conduction-band transitions. The free-electron contribution to $\epsilon_2$ at the 5-eV peak is zero; thus, the only contribution to the peak is represented in the joint density of states. It is therefore possible to obtain an approximate value for $M_{vc}$ using the relation

$$\epsilon_2(5\text{ eV}) = C|M_{vc}|^2 J(5\text{ eV})/\omega^2, \qquad (5)$$

where $\epsilon_2(5\text{ eV})$ is obtained from the optical data and $J(5\text{ eV})$ is from the JDOS calculations. Thus the ratio $|M_{cc}|^2/|M_{vc}|^2$ can be determined. Since the valence and conduction bands are predominantly $p$-like and $d$-like, respectively, the matrix element $M_{cc}$ is expected to be smaller than $M_{vc}$, as dipole selection rules do not allow $d$ to $d$ transitions. However, some mixing occurs in the bands and transitions within the conduction band are not necessarily eliminated.

The analysis was carried out for the composition $x = 0.94$, using the JDOS calculations for $x = 0.9$. Equation (1) for $\epsilon_1$ and Eq. (4) for $\epsilon_2$, were fit to the data simultaneously using various values of $M_{cc}$. It was found that a reasonable fit to the data could be obtained for values of $|M_{cc}|^2/|M_{vc}|^2$ from 0 to 0.15. A typical curve is shown in Fig. 8. The contribution from the direct transitions and the Drude component are shown along with the sum of the two. The parameters obtained are summarized in Table I, where the first line of the table contains the values obtained from the Drude model alone. As the matrix element $M_{cc}$ increases, $\tau$ also increased, bringing it in better agreement with the dc value. The matrix elements for the transitions within the conduction band are considerably lower than those for the valence- to conduction-band transitions, as expected.

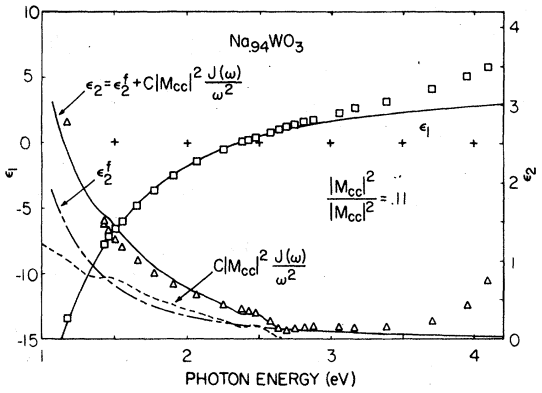


FIG. 8. Free-electron model (short-dashed line) combined with interband contributions to $\epsilon_2$ obtained from JDOS calculations (short–long-dashed line). The solid line is the sum of the free- and bound-electron contributions.

TABLE I.

| $\lvert M_{cc}\rvert^2/\lvert M_{vc}\rvert^2$ | $\tau(\times 10^{-14}$ sec) | $m^*/m_0$ | $\epsilon_1^b$ |
|---|---|---|---|
| 0 | 0.37 | 0.89 | 3.4 |
| 0.06 | 0.53 | 0.89 | 3.5 |
| 0.11 | 0.73 | 0.89 | 3.5 |
| 0.15 | 1.20 | 0.89 | 3.5 |

One interesting aspect of Fig. 8 is the "dip" in $\epsilon_2$ which the JDOS calculations produce at 2.6 eV. It coincides remarkably well with structure in the data. However, when the reflectivity is extremely low, as it is in this region, surface structure can produce artifacts in the data, and it would be premature to attach a great deal of significance to this agreement.

### C. Determination of $\epsilon_1^b$ using $WO_3$ dielectric constants

In fitting the optical data to the free-electron model as described in the previous sections it was assumed that $\epsilon_1^b$, the contribution to the real part of the dielectric constant from the higher-energy transitions, was constant with wavelength for each composition. There are a number of methods by which the wavelength dependence of $\epsilon_1^b$ might be included, one of which is to attempt to fit the entire spectrum to a model containing free-electron and bound-electron Lorentz oscillator terms. This was done using a single Lorentz oscillator in addition to the Drude term. As might be expected, a single oscillator does not adequately describe optical structure which does not result from a discrete transition but, in fact, originates from

a number of closely spaced transitions. Consequently, in the high-energy range the data fit the model poorly. Another approach for including the frequency dependence of $\epsilon_1^b$ in the free-electron model is to use the optical dielectric constants of the tungsten-bronze host lattice, $WO_3$, to determine $\epsilon_1^b$ directly. If the rigid-band model for the system is a good approximation, the optical constants of $WO_3$ should be identical to those of $Na_xWO_3$ without the free-electron contribution and therefore could be subtracted from the $Na_xWO_3$ data to yield the free-electron optical constants. These optical constants could then be analyzed in terms of the Drude model. The situation is somewhat complicated by the fact that $WO_3$ does not have the same crystal structure or lattice spacing as $Na_xWO_3$. The $WO_3$ data are, however, remarkably similar to the $Na_xWO_3$ results, indicating that the procedure is a good first approximation, if one accounts for the shift in the uv structure in $Na_xWO_3$ and $WO_3$.

In order to account for the shift of the uv structure, the $WO_3$ data was first fit to a single-oscillator Lorentz function with the resonant frequency chosen to correspond to the $\epsilon_2$ peak in the $WO_3$ spectrum. The function fits the long-wavelength data, which is all that is of interest in this case, reasonably well. The parameters obtained were then used to calculate $\epsilon_1^b$, the bound-electron contribution, for $Na_xWO_3$ by changing the value of the resonant frequency to correspond to the peak in $\epsilon_2$ for the particular sodium-bronze sample being analyzed. As expected, the contribution was very flat in the long-wavelength region and did not deviate by more than 15% from the values obtained when $\epsilon_1^b$ was entered in the model as a frequency-independent fitting parameter. A least-squares fit of the $Na_xWO_3$ data to the functions in Eqs. (1) and (2), with $\epsilon_1^b$ replaced by $\epsilon_1^b(\omega)$ yields results almost identical to those discussed in Sec. IV A. The values obtained for $m^*/m_0$ and $\tau$ are shown as a function of composition in Fig. 6. The similarity of the results substantiates the initial assumption that $\epsilon_1^b$ is relatively wavelength independent in the free-electron region and also gives further evidence of the rigid-band nature of the system.

## V. CONCLUSION

The optical data support the assumption that the sodium-tungsten bronzes are an almost rigid-band system. Because of this rigid-band behavior optical data from $WO_3$ can be used in conjunction with the Drude free-electron model to separate the free- and bound-electron contributions to the dielectric constants of $Na_xWO_3$. Although the parameters determined from the model vary with composition in a manner which would be expected from consideration of the band structure, the absolute value of the relaxation time obtained is about a factor of 3 lower than that extracted from the dc conductivity. By including in the classical free-electron model a contribution to the optical constants calculated from recently obtained joint density of states functions, with the matrix element as a fitting parameter, agreement between the dc and optical relaxation times is obtained with a reasonable value of the matrix element and a good fit to the data. Thus we conclude that direct transitions within the conduction band may make a significant contribution to the discrepancy between the electron relaxation time determined from the "free-electron" optical properties and relaxation time obtained from the dc conductivity.

## ACKNOWLEDGMENTS

The authors wish to express appreciation to B. N. Harmon for providing the unpublished JDOS calculations used in the analysis and for a number of helpful discussions, and to E. M. Brody for consultation during the course of the investigation. We also wish to thank I. Chabay for advice in the construction of the optical modulator. This work was supported in part by the U. S. Department of Energy, Office of Basic Energy Sciences, Materials Sciences Division. One of us, (J.F.O.) would like to thank the American Can Company for support through a Materials Science Fellowship during this work.

[1]For a review of the bronzes, see M. J. Sienko, Adv. Chem. Ser. 39, 224 (1963); H. R. Shanks, P. H. Sidles, and G. C. Danielson, Adv. Chem. Ser. 39, 237 (1962); P. G. Dickens and M. S. Whittingham, Q. Rev. Chem. Soc. 22, 30 (1968).

[2]B. W. Brown and E. Banks, J. Am. Chem. Soc. 76, 963 (1954).

[3]J. H. Ingold and R. C. Devries, Acta Metall. 6, 736 (1958).

[4]P. G. Dickens, R. M. P. Quilliam, and M. S. Whittingham, Mater. Res. Bull. 3, 941 (1968).

[5]G. H. Taylor, J. Solid State Chem. 1, 359 (1969).

[6]S. Fujieda, Sci. Light (Tokyo) 18, 1 (1969).

[7]J. Feinleib, W. J. Scouler, and A. Ferretti, Phys. Rev. 165, 765 (1968).

[8]J. H. Weaver and D. W. Lynch, Phys. Rev. B 6, 3620 (1972).

[9]F. Consadori and A. Stella, Lett. Nuovo Cimento 3, 600

(1970).
[10]G. Giuliani, A. Gustinetti, and A. Stella, Phys. Lett. A 38, 515 (1972).
[11]D. W. Lynch, R. Rosei, J. H. Weaver, and C. G. Olson, J. Solid State Chem. 8, 242 (1973).
[12]P. Camagni, A. Manara, G. Campagnoli, A. Gustinetti, and A. Stella, Phys. Rev. B 15, 4623 (1977).
[13]B. N. Harmon (unpublished work). The JDOS calculations were made by fitting the $Na_xWO_3$ electronic bands to Fourier series and using a tetrahedron method [G. Lehmann and M. Taut, Phys. Status Solidi 54, 469 (1972)] for performing the Brillouin-zone integration.
[14]S. N. Jasperson and S. E. Schnatterly, Rev. Sci. Instrum. 10, 761 (1969).
[15]S. Sawada and G. C. Danielson, Phys. Rev. 113, 1008 (1959).
[16]R. H. W. Graves, J. Opt. Soc. Am. 59, 1225 (1969).
[17]I. Chabay, E. C. Hsu, and G. Holzwarth, Chem. Phys. Lett. 15, 211 (1972).
[18]H. R. Shanks, J. Cryst. Growth 13/14, 433 (1972).
[19]R. J. Reuland and A. F. Voigt, Anal. Chem. 35, 1263 (1963).
[20]S. Sawada and G. C. Danielson, Phys. Rev. 113, 1005 (1959).
[21]L. Kopp, B. N. Harmon, and S. H. Liu, Solid State Commun. 22, 677 (1977).
[22]L. F. Mattheiss, Phys. Rev. 181, 181 (1969).
[23]L. F. Mattheiss, Phys. Rev. B 2, 3918 (1970).
[24]J. B. Goodenough, Prog. Solid State Chem. 5, 145 (1971).
[25]M. Campagna, G. K. Wertheim, H. R. Shanks, F. Zumsteg, and E. Banks, Phys. Rev. Lett. 34, 738 (1975).
[26]L. D. Muhlestein and G. C. Danielson, Phys. Rev. 158, 825 (1967).
[27]J. D. Greiner, H. R. Shanks, and D. C. Wallace, J. Chem. Phys. 36, 772 (1962).
[28]B. L. Crowder and M. J. Sienko, J. Chem. Phys. 38, 1576 (1963).
[29]R. W. Vest, M. Griffel, and J. F. Smith, J. Chem. Phys. 28, 293 (1958).
[30]H. Ehrenreich and H. R. Philipp, Phys. Rev. 128, 1622 (1962).
[31]H. Ehrenreich, H. R. Philipp, and B. Segall, Phys. Rev. 132, 1918 (1963).
[32]N. Smith, Phys. Rev. 183, 634 (1969).
[33]M. Thèye, Phys. Rev. B 2, 3060 (1970).
[34]F. Abelès, in *Optical Properties of Solids*, edited by F. Abelès (North-Holland, Amsterdam, 1972), p. 93.
[35]T. Holstein, Phys. Rev. 96, 535 (1954).
[36]R. N. Gurzhi, Sov. Phys.-JETP 8, 673 (1959).